Chemical Physics Letters 485 (2010) 59–63

Contents lists available at ScienceDirect

Chemical Physics Letters

journal homepage: www.elsevier.com/locate/cplett

Time-resolved dynamics in acetonitrile cluster anions $(CH_3CN)_n^-$

Ryan M. Young [a], Graham B. Griffin [a], Aster Kammrath [a,b], Oli T. Ehrler [a,c], Daniel M. Neumark [a,d,*]

[a] Department of Chemistry, University of California, Berkeley, CA 94720, USA
[b] Department of Chemistry, University of Wisconsin, Madison, WI 53706, USA
[c] Department of Chemistry, Karlsruhe Institute of Technology, Karlsruhe, Germany
[d] Chemical Sciences Division, Lawrence Berkeley National Laboratory, Berkeley, CA 94720, USA

ARTICLE INFO

Article history:
Received 11 November 2009
In final form 17 December 2009
Available online 23 December 2009

ABSTRACT

Excited state dynamics of acetonitrile cluster anions, $(CH_3CN)_n^-$, were investigated using time-resolved photoelectron imaging (TRPEI) for $20 \leqslant n \leqslant 50$. The clusters were excited and then photodetached with femtosecond pump and probe pulses at 790 and 395 nm, respectively. Excited state lifetimes varied between 200 and 270 fs over this size range, showing no obvious size trend. Experimental evidence indicates that we are exciting 'isomer II' clusters in which the excess electron is valence-bound to a solvated anionic dimer core. The absence of an obvious size-dependence in the excited state lifetimes is consistent with such a structure.

1. Introduction

Solvated electrons are important species in chemistry, biology, and physics. A solvated electron is a purely quantum mechanical solute and is therefore of fundamental interest in condensed phase chemistry. From a more practical perspective, solvated electrons are formed by ionizing radiation and are thus key players in radiation chemistry and biology [1,2]. While much interest has focused on hydrated electrons [3], i.e. electrons in aqueous solution, solvated electrons have been observed in numerous inorganic and organic solvents. The properties of solvated electrons depend significantly on the solvent in which they are formed, and the nature of the electron–solvent interaction responsible for these properties has been the focus of numerous experimental and theoretical studies. Many aspects of the electron–solvent interaction are controversial. Even in water, the most thoroughly studied solvent, unresolved questions remain concerning structural issues centered on whether the electron exists in a solvent cavity [4] or in a chemically bound form [5], as well as dynamical issues related to the mechanism by which delocalized and/or electronically excited electrons relax to their ground state [6].

These considerations have motivated studies of gas phase clusters of the type S_n^-, in which an excess electron is bound to a known number of solvent species S, with the goal of applying the powerful experimental tools developed for gas phase spectroscopy and dynamics to these clusters and then extrapolating the results to the infinite size limit to shed light on the properties of electrons in bulk solvents [7]. Several laboratories have reported one-photon [8–11] and time-resolved [12–14] photoelectron (PE) spectra of $(H_2O)_n^-$ clusters, while we have carried out both types of studies on $(CH_3OH)_n^-$ clusters [15,16]. This line of inquiry is continued in this Letter, where we report time-resolved PE spectra for $(CH_3CN)_n^-$ clusters.

Electrons dissolved in bulk CH_3CN show two broad absorption bands, one in the near-infrared, peaking from 1200 to 1400 nm, and the other in the visible around 500 nm [17]. Recent studies by Shkrob and Sauer [18] and Kohler [19] have attributed the near-IR band to a solvated electron located within a solvent cavity, and the visible band to an electron localized on a monomer or (more likely) a dimer of CH_3CN. The dimer unit, $(CH_3CN)_2^-$, is a valence-bound species in which the excess electron is distributed over the π^* orbitals of two bent, antiparallel solvent molecules [19,20].

Evidence for two electron solvation motifs in acetonitrile also comes from PE spectra of $(CH_3CN)_n^-$ ($n = 10$–100) clusters measured by Kaya and co-workers [21]. These show the existence of two cluster isomers: a weakly bound isomer (isomer I) with vertical detachment energies (VDE's) ranging from 0.4 to 1.0 eV, and a more strongly bound isomer (isomer II) with VDE's from 2.2 to 2.8 eV. Isomer II dominates starting at $n = 13$, but both are seen out to $n = 100$. Based on comparison with the bulk results, isomer II was attributed to clusters with a valence-bound, $(CH_3CN)_2^-$ core, while the more weakly bound isomer I was assigned to an electron within a solvent cavity. Recent electronic structure calculations [20,22] on small $(CH_3CN)_n^-$ clusters support the existence of the two isomers along these lines. The calculations by Takayanagi et al. [22] are particularly relevant as they show that the $(CH_3CN)_2^-$ anion core, which is unstable in the gas phase with

* Corresponding author. Address: Department of Chemistry, University of California, B64 Hildebrand Hall, Berkeley, CA 94720, USA. Fax: +1 510 642 3635.
E-mail address: dneumark@berkeley.edu (D.M. Neumark).

0009-2614/$ - see front matter © 2009 Elsevier B.V. All rights reserved.
doi:10.1016/j.cplett.2009.12.058

respect to autodetachment, becomes thermodynamically stable with the addition of only a few solvent molecules.

Time-resolved experiments on electrons in liquid acetonitrile were performed by Kohler [19], who excited the charge-transfer-to-solvent (CTTS) band of the iodide anion in CH_3CN at 265 nm and monitored the resulting electron solvation dynamics with transient absorption. The overall dynamics were described by three time-constants, 1.9, 29, and 257 ps, attributed respectively to initial solvation dynamics, geminate recombination of the free electron with the I atom, and scavenging of the electron by CH_3CN monomer or dimer. The cluster analog to this experiment was performed in our group [23,24], in which we measured time-resolved PE spectra of $I^-(CH_3CN)_n$ clusters subsequent to ejection of the electron from the iodide to the surrounding solvent network. The VDE dropped abruptly within 300–400 fs, followed by a bi-exponential increase that was complete by ~10 ps. Previous theoretical work [25] found that the iodide is internally solvated, and that photodetachment results in formation of a diffuse electron cloud in a confined cavity. We interpreted the initial drop in VDE as a combination of expansion of the cavity and localization of the excess electron on one or two solvent molecules. The subsequent increase in VDE was attributed to a combination of the I atom leaving the cavity and rearrangement of the acetonitrile molecules to solvate the electron.

In this Letter, we use time-resolved photoelectron imaging (TRPEI) [26] to investigate the relaxation dynamics of electronically excited $(CH_3CN)_n^-$ isomer II clusters in the size range $n = 20$–50. These experiments complement our previous work on $I^-(CH_3CN)_n$ clusters, in the same way that our TRPEI studies on $I^-(H_2O)_n$ and $(H_2O)_n^-$ clusters complemented one another [27]. There is reasonably strong evidence that in CH_3CN clusters, both the iodide and excess electron are internally solvated [20,22,25,28,29]. In contrast, small water clusters ($n \leqslant 25$) favor surface solvation for both species [30,31], while the nature of electron solvation in larger clusters is being actively investigated [11,32,33]. Hence, the experiments presented here provide an opportunity to investigate the dynamics of internally solvated electrons and to compare the results to other solvent clusters where the solvation motif is less settled. We find that the excited state of isomer II after 790 nm excitation has a lifetime of 200–270 fs for the size range studied here with no obvious dependence on cluster size. The absence of size-dependence is consistent with the assignment of isomer II as a having a valence-bound anion core solvated by the remaining solvent molecules.

2. Experimental

Details of our experiment setup have been presented previously [34]; only a brief summary will be given here. A seeded supersonic expansion was created by passing argon gas at 35 psig over room temperature liquid acetonitrile. The resulting gas mixture was sent through a solenoid valve [35] pulsed at 87 Hz into the vacuum chamber. Anion clusters were formed by secondary electron attachment to neutral $(CH_3CN)_n$ clusters [36] from a pulsed ring ionizer attached to the valve. The resulting anions were extracted perpendicularly into a Wiley–McLaren time-of-flight mass spectrometer [37] where ions of the desired mass were transmitted by an electrostatic switch pulsed at the appropriate time. This ion packet was interrogated by femtosecond pump and probe laser pulses that induced electronic excitation and photodetachment, respectively. The detached photoelectrons were accelerated by velocity-map imaging [38] onto microchannel plates coupled to a phosphor screen. A CCD camera converted this to a digital image that was four-way symmetrized and inverted using the BASEX method [39] to recover the photoelectron velocity distribution.

Photoelectron kinetic energy spectra were obtained via angular integration. The images also yielded photoelectron angular distributions (PADs) as a function of electron kinetic energy (eKE), which, for one-photon processes, are given by [40]

$$I(\theta, eKE; n) = \frac{\sigma_{\text{total}}}{4\pi}[1 + \beta(eKE; n)P_2(\cos\theta)], \quad (1)$$

where θ is the angle between the emitted electron and the laser polarization, n is the cluster size, σ_{total} is the total photodetachment cross section, and β is the anisotropy parameter for the feature of interest.

The pump and probe laser pulses were created by a commercial Ti:sapphire femtosecond oscillator and amplified by chirped-pulse multipass amplification (KM Labs Griffin oscillator/Dragon amplifier), yielding pulses at a center wavelength of 790 nm (1.57 eV) with a pulse duration of 35 fs. Some of this light was directed through a BBO crystal to generate probe pulses at the second harmonic wavelength, 395 nm (3.14 eV), yielding 120 μJ pulses with minimal temporal broadening. The remaining fundamental was attenuated to <20 μJ/pulse and used as the pump. The cross-correlation time within the vacuum chamber was ~70 fs FWHM as measured separately by above-threshold detachment of negative ions.

3. Results and analysis

Reconstructed single photon photoelectron images and their associated normalized kinetic energy spectra are shown in Fig. 1 for $(CH_3CN)_{40}^-$. Kinetic energy spectra are shown in Fig. 1a for photon energies $h\nu = 1.57$ eV (red) and $h\nu = 3.14$ eV (blue). The red curve in Fig. 1a is multiplied by a factor of 20. Fig. 1b and c show the associated photoelectron Newton spheres for the red and blue curves, respectively.

For photodetachment at 1.57 eV, peak B, centered at an eKE of 1.0 eV, is from direct detachment of isomer I. Peak C, seen from photodetachment at 3.14 eV, is from direct detachment of isomer II; these features yield VDE's of 0.6 and 2.6 eV for isomers I and II, respectively. At 3.14 eV, virtually no signal is seen from isomer I for this cluster size. The very slow peak A is attributed to vibrational autodetachment of isomer II excited at 1.57 eV, since this photon energy lies well above the VDE of isomer I. While the energetics and relative isomer intensities are consistent with the PE spectra measured by Kaya at 3.50 eV [21], the slow autodetachment feature was not seen previously; its observation here results from using photoelectron imaging for detection, which is considerably more

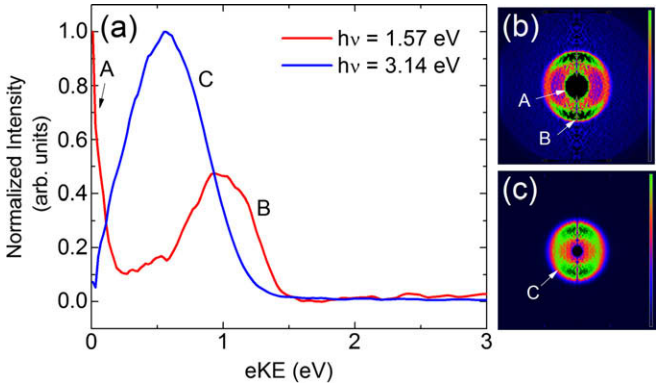

Fig. 1. (a) One-photon photoelectron spectra of $(CH_3CN)_{40}^-$ taken at $h\nu = 1.57$ eV (red) and 3.14 eV (blue). The red spectrum is scaled up by a factor of 20. Feature A is excited state autodetachment from isomer II and feature B is direct detachment of isomer I. Feature C, at 3.14 eV, is from direct detachment of isomer II. BASEX reconstructed photoelectron Newton spheres are shown at (b) $h\nu = 1.57$ eV and (c) $h\nu = 3.14$ eV, with the intensity of image (b) scaled up by a factor of 5. See text for details and extracted anisotropy parameters.

sensitive to slow electrons than time-of-flight photoelectron spectroscopy. The photoelectron image for feature B from isomer I shows significant anisotropy in the PAD. We find that $\beta_B = 0.60 \pm 0.07$ for the outer feature. Isomer II has a more symmetric photoelectron image, with feature C having $\beta_C = 0.35 \pm 0.09$.

Time-resolved photoelectron images of $(CH_3CN)_n^-$ were recorded for $20 \leqslant n \leqslant 50$, with pump and probe-photon energies of 1.57 and 3.14 eV, respectively. Representative photoelectron spectra for $n = 39$ extracted from these images are displayed in Fig. 2, with pump–probe delay increasing nonlinearly from back to front and feature C scaled down by a factor of 8. These spectra show a weak, short-lived transient between 2.4 and 3.4 eV, feature D, attributed to excited state dynamics induced by the pump pulse.

The intensity of the excited state feature D is shown in Fig. 3, integrated from 2.45 to 3.20 eV. The fitting procedure involves convoluting an exponential decay with lifetime τ beginning at t_0,

$$P(t) = \begin{cases} I_0 & t < t_0, \\ I_0 + A_1 e^{-t/\tau} & t \geqslant t_0, \end{cases} \quad (2)$$

with a Gaussian instrument response function of width σ (given by FWHM = $2\sigma\sqrt{2\ln 2}$), yielding [41,42]

$$I(t) = I_0 + A_2 \left\{ 1 - \mathrm{erf}\left(\frac{\sigma}{2\tau} - \frac{t - t_0}{\sigma} \right) \right\} e^{\left[\left(\frac{\sigma}{2\tau}\right)^2 - \frac{t-t_0}{\tau} \right]}, \quad (3)$$

where the A's are scaling factors and I_0 is an offset. Integration is performed on the higher eKE side of feature D in order to minimize contamination from isomer I, from which instrument-limited above-threshold detachment can occur and obscure the dynamics. The extracted decay constant for the excited state in $n = 39$ is $\tau = 226 \pm 19$ fs. Excited state lifetimes as a function of cluster size are shown in Fig. 4; each point is the average of multiple experiments on the same cluster size, with the error bars representing the standard deviation of the mean, or in the case of only a single data set, the standard error associated with the fit. The lifetime of the excited state is relatively constant over the cluster size range, varying from 208 to 266 fs, with no clear size-dependent trend.

Peak C, from probe-photon detachment of isomer II, exhibits a small but rapid decrease at positive pump–probe delays, displayed in the inset of Fig. 3, showing that the probe pulse depletes the ground state population of isomer II. It is unclear if there is any

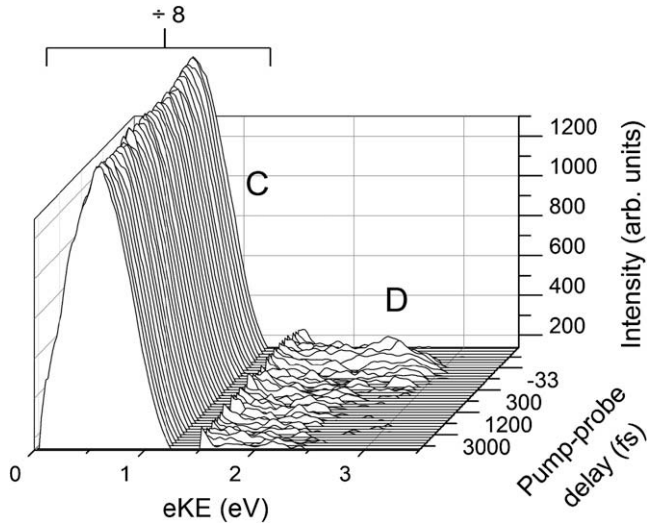

Fig. 2. Time-resolved photoelectron spectra displayed as a waterfall plot for $(CH_3CN)_{39}^-$ with $h\nu_{pump} = 1.57$ eV and $h\nu_{probe} = 3.14$ eV, with pump–probe delay increasing from front to back. The time-dependent feature D occurs at the zero of pump–probe delay, in the energy range 2.45–3.20 eV. Feature C is scaled down by a factor of 8.

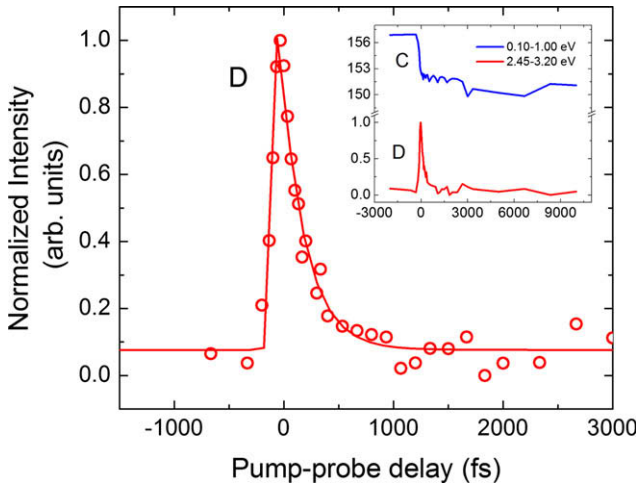

Fig. 3. Integrated intensity for $(CH_3CN)_{39}^-$ feature D upon 1.57 eV excitation. Data are integrated from 2.45 to 3.20 eV. The excited state reaches its maximum shortly after t_0, and decays back to its initial value with a time constant of $\tau = 226 \pm 19$ fs. Inset: depletion of feature C, normalized to the maximum of feature D, showing no recovery out to 10 ps.

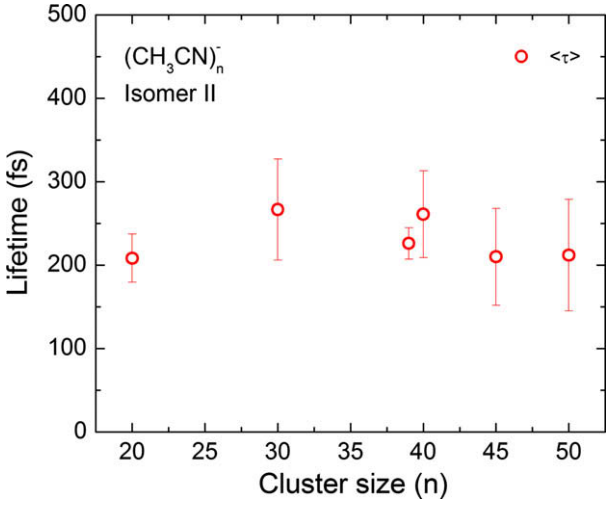

Fig. 4. Isomer II excited state lifetime as a function of cluster size. All timescales reported lie between 200 and 270 fs.

recovery of the ground state population for larger cluster sizes; recovery has been observed for $n \geqslant 40$, but the signal is not reproducible in every experiment, most likely reflecting the difficulty in accurately measuring a small pump-induced depletion signal (~2%, see inset of Fig. 3) on top of a large background.

4. Discussion

The one-photon photoelectron kinetic energy spectra in Fig. 1 and the time-resolved photoelectron spectra can be interpreted with reference to Fig. 5, which shows the vertical detachment energy for isomer II of $(CH_3CN)_{40}^-$. Isomer I is not shown on this diagram, because its energetics relative to isomer II are unknown. While the difference in the VDE's between the two isomers is known, vertical detachment accesses rather different neutral species in each case; the two bent CH_3CN molecules comprising the dimer anion core in isomer II represent a particularly high energy configuration for the neutral cluster, for example. The photoelectron spectrum associated with isomer II (peak C, Fig. 1) is superimposed on this diagram, and

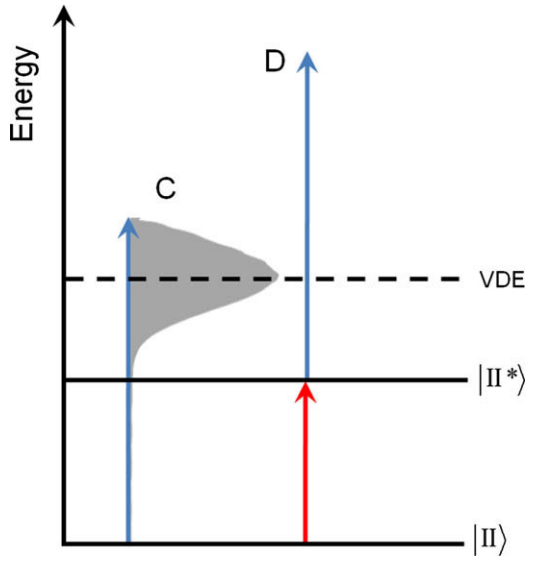

Fig. 5. Energetics for electronic states of isomer II in $(CH_3CN)_{40}^-$, with photoelectron spectrum from Fig. 1 at 3.14 eV superimposed. State II* is formed by excitation at 1.57 eV. Autodetachment from this state is energetically allowed.

as such it represents the spectrum of electron binding energies given by hν-eKE. Note that this spectrum extends down to 1.57 eV, the photon energy used to generate the red spectrum in Fig. 1. Hence, an excited state of isomer II produced at this photon energy will have sufficient energy to undergo autodetachment, producing the very slow electrons (peak A) in Fig. 1.

The one-photon images in Fig. 1b and c provide additional insight into the nature of the excess electron in isomers I and II of $(CH_3CN)_n^-$ clusters. The PAD's associated with detachment from the two isomers are distinctly different, with peak B from isomer I showing more anisotropy than peak C from isomer II ($\beta_C = 0.60 \pm 0.07$ vs. 0.35 ± 0.09). The PAD is sensitive to the shape of the orbital from which detachment occurs [43], so our results are consistent with quite different electronic wavefunctions for the excess electron in the two isomers. Moreover, the more positive value of β for isomer I suggests more s-like character for the excess electron than in isomer II, which is again consistent with the notion that the excess electron in isomer I resides in a solvent cavity as opposed to a more structured π^* orbital expected for localization on a CH_3CN dimer unit [20]. Hence, the PAD's offer some support for previous assignments of the two isomers.

We next consider the interpretation of the transient feature D in our experiments. The pump laser wavelength of 790 nm is on the red edge of the electronic absorption band of electrons in liquid acetonitrile localized on solvent dimers [17,19]. Since this dimer-localized motif is calculated to lie at the core of isomer II cluster anions [22], it is reasonable to assign feature D to pump–probe signal via the isomer II excited state, labeled II* in Fig. 5, and its decay to the lifetime of this excited state. Several specific observations from our results support this interpretation. First, the observation of autodetachment (Fig. 1) implies that the 790 nm pump pulse overlaps an electronic transition of $(CH_3CN)_{40}^-$. Secondly, while the measured lifetime of feature D is quite short, ~200 fs over the size range considered here, it is significantly longer than the temporal width of the laser pulses (~70 fs). This measurement therefore rules out feature D originating from, for example, two-color above-threshold detachment of isomer I or isomer II, since either process would result in symmetric transients persisting only during the cross-correlation of the pump and probe laser pulses. Finally, the pump-induced depletion of peak C, the isomer II ground state feature, for all clusters shows that the pump pulse is exciting isomer II. This result also confirms the proposed association of the bulk 500 nm electronic transition with isomer II [21].

The excited state lifetimes for $n = 20$–50 shown in Fig. 4 all lie between 200 and 270 fs and show no obvious size-dependence. This result differs from the excited state lifetimes in comparably-sized water cluster anions [13] which, for example, drop from 400 fs for $(D_2O)_{25}^-$ to 200 fs for $(D_2O)_{50}^-$. Such a result is consistent with the attribution of isomer II clusters built around a valence-bound $(CH_3CN)_2^-$ dimer core, whose properties are relatively insensitive to solvent molecules beyond those in direct contact with this moiety. The calculations by Takayanagi et al. [22] find that in isomer II of $(CH_3CN)_8^-$, there are three solvent molecules bound to each N atom of the dimer anion core, and eight molecules on each core N atom for $(CH_3CN)_{10}^-$. The first solvent shell would continue to build in this manner until it is closed, encapsulating the dimer anion. Over the size range studied here, it is reasonable to assume that the number of strong binding sites on the dimer core is saturated.

While our experiments yield excited state lifetimes, the relaxation pathway for the cluster excited state is less clear. In water cluster anions, the time-constants for excited state decay and ground state recovery were nearly the same over a wide cluster size range [13,42], indicating that the excited state decayed by internal conversion to the ground state. The situation is more complicated for acetonitrile, given that no recovery of the ground state feature C is seen for cluster sizes below $n = 40$. While there are hints of recovery for larger clusters, we have not been able to observe this reliably. We also searched for recovery in the energy region where probe-induced detachment from isomer I would occur, around 2.4–2.5 eV, with the idea that isomer I might be formed as an intermediate decay product from the excited state II*, but no evidence for this was seen, either. It is possible that excited state autodetachment is the primary decay channel for state II*. This channel is open, as evidenced by peak A, and autodetachment was observed to compete with internal conversion for excited $(H_2O)_n^-$ clusters with $n < 25$, although the autodetachment yield never exceeded 25% [42]. Future studies on larger clusters than those reported here at wavelengths closer to the bulk absorption band at 500 nm may provide additional insights into the excited state decay channels.

The results presented here show that the excited state decay dynamics in $(CH_3CN)_n^-$ clusters are quite different from those in water and methanol cluster anions [27], showing a much weaker and possibly non-existent size-dependence in the $n = 20$–50 size regime. It will be of considerable interest to see if these lifetimes carry over into electrons in liquid acetonitrile, and we hope our results will stimulate such investigations in other laboratories.

5. Conclusions

Time-resolved photoelectron imaging was used to investigate excited state dynamics in acetonitrile cluster anions $(CH_3CN)_n^-$ over the size range $20 \leqslant n \leqslant 50$. These experiments were performed using femtosecond pump and probe laser pulses at 790 and 395 nm, respectively, in which the pump pulse electronically excited the clusters and the probe pulse photodetached them. In this cluster size regime, isomer II cluster anions, in which the excess electron is valence-bound to a solvated dimer anion core, are the dominant species. We observed pump–probe signal yielding excited state lifetimes of isomer II clusters with decay times varying between 208 fs and 266 fs with no obvious size-dependent trend. Depletion of the ground state population was observed for all clusters, which signifies that the visible absorption band in the bulk is associated with isomer II, as proposed in the literature. The absence of a clear size-dependence, in contrast to earlier work on

water and methanol cluster anions, is consistent with a highly localized excess electron that is only weakly perturbed by solvent molecules beyond the first solvation shell.

Acknowledgements

This work was supported by the National Science Foundation (CHE-0649647). The authors thank Markus Niemeyer and Maggie Yandell for their assistance. OTE acknowledges the Alexander von Humboldt Foundation for a Feodor-Lynen Fellowship.

References

[1] D.M. Bartels, A.R. Cook, M. Mudaliar, C.D. Jonah, J. Phys. Chem. A 104 (2000) 1686.
[2] J. Simons, Chem. Res. 39 (2006) 772.
[3] E.J. Hart, M. Anbar, The Hydrated Electron, Wiley-Interscience, New York, 1970.
[4] P.J. Rossky, J. Schnitker, J. Phys. Chem. 92 (1988) 4277.
[5] H.F. Hameka, G.W. Robinson, C.J. Marsden, J. Phys. Chem. 91 (1987) 3150.
[6] C. Silva, P.K. Walhout, K. Yokoyama, P. Barbara, Phys. Rev. Lett. 80 (1998) 1086.
[7] J.V. Coe, S.M. Williams, K.H. Bowen, Int. Rev. Phys. Chem. 27 (2008) 27.
[8] J.V. Coe et al., J. Chem. Phys. 92 (1990) 3980.
[9] J. Kim, I. Becker, O. Cheshnovsky, M.A. Johnson, Chem. Phys. Lett. 297 (1998) 90.
[10] J.R.R. Verlet, A.E. Bragg, A. Kammrath, O. Cheshnovsky, D.M. Neumark, Science 307 (2005) 93.
[11] L. Ma, K. Majer, F. Chirot, B.V. Issendorff, J. Chem. Phys. 131 (2009) 144303.
[12] J.M. Weber, J. Kim, E.A. Woronowicz, G.H. Weddle, I. Becker, O. Cheshnovsky, M.A. Johnson, Chem. Phys. Lett. 339 (2001) 337.
[13] A.E. Bragg, J.R.R. Verlet, A. Kammrath, O. Cheshnovsky, D.M. Neumark, Science 306 (2004) 669.
[14] D.H. Paik, I. Lee, D. Yang, J.S. Baskin, A.H. Zewail, Science 306 (2004) 672.
[15] A. Kammrath, J.R.R. Verlet, G.B. Griffin, D.M. Neumark, J. Chem. Phys. 125 (2006) 171102.
[16] A. Kammrath, G.B. Griffin, J.R.R. Verlet, R.M. Young, D.M. Neumark, J. Chem. Phys. 126 (2007) 244306.
[17] I.P. Bell, M.A.J. Rodgers, H.D. Burrows, Chem. Soc. Faraday Trans. I 73 (1977) 315.
[18] I.A. Shkrob, M.C. Sauer, J. Phys. Chem. A 106 (2002) 9120.
[19] C.G. Xia, J. Peon, B. Kohler, J. Chem. Phys. 117 (2002) 8855.
[20] Q.K. Timerghazin, G.H. Peslherbe, J. Phys. Chem. B 112 (2008) 520.
[21] M. Mitsui, N. Ando, S. Kokubo, A. Nakajima, K. Kaya, Phys. Rev. Lett. 91 (2003) 153002.
[22] T. Takayanagi, T. Hoshino, K. Takahashi, Chem. Phys. 324 (2006) 679.
[23] O.T. Ehrler, G.B. Griffin, R.M. Young, D.M. Neumark, J. Phys. Chem. B 113 (2009) 4031.
[24] O.T. Ehrler, D.M. Neumark, Acc. Chem. Res. 42 (2009) 769.
[25] T. Takayanagi, Phys. Chem. A 110 (2006) 7011.
[26] A. Stolow, A.E. Bragg, D.M. Neumark, Chem. Rev. 104 (2004) 1719.
[27] D.M. Neumark, Mol. Phys. 106 (2008) 2183.
[28] G. Markovich, L. Perera, M.L. Berkowitz, O. Cheshnovsky, J. Chem. Phys. 105 (1996) 2675.
[29] T.N.V. Nguyen, G.H. Peslherbe, J. Phys. Chem. A 107 (2003) 1540.
[30] D.M. Koch, G.H. Peslherbe, Chem. Phys. Lett. 359 (2002) 381.
[31] J.R. Roscioli, N.I. Hammer, M.A. Johnson, J. Phys. Chem. A 110 (2006) 7517.
[32] K.R. Asmis et al., J. Chem. Phys. 126 (2007) 191105.
[33] A. Madarasz, P.J. Rossky, L. Turi, J. Chem. Phys. 130 (2009).
[34] A.V. Davis, R. Wester, A.E. Bragg, D.M. Neumark, J. Chem. Phys. 118 (2003) 999.
[35] U. Even, J. Jortner, D. Noy, N. Lavie, C. Cossart-Magos, J. Chem. Phys. 112 (2000) 8068.
[36] K. Mitsuke, T. Kondow, K. Kuchitsu, J. Phys. Chem. 90 (1986) 1505.
[37] W.C. Wiley, I.H. McLaren, Rev. Sci. Instrum. 26 (1955) 1150.
[38] A.T.J.B. Eppink, D.H. Parker, Rev. Sci. Instrum. 68 (1997) 3477.
[39] V. Dribinski, A. Ossadtchi, V.A. Mandelshtam, H. Reisler, Rev. Sci. Instrum. 73 (2002) 2634.
[40] J. Cooper, R.N. Zare, J. Chem. Phys. 48 (1968) 942.
[41] T.E. Dermota, D.P. Hydutsky, N.J. Bianco, A.W. Castleman, J. Phys. Chem. A 109 (2005) 8254.
[42] G.B. Griffin, R.M. Young, O.T. Ehrler, D.M. Neumark, J. Chem. Phys. 131 (2009) 194302.
[43] K.L. Reid, Annu. Rev. Phys. Chem. 54 (2003) 397.